Geosci. Instrum. Method. Data Syst. Discuss., https://doi.org/10.5194/gi-2018-47
Manuscript under review for journal Geosci. Instrum. Method. Data Syst.
Discussion started: 2 October 2018

Geoscientific Instrumentation Methods and Data Systems Discussions
Open Access

Integration of Remote Sense and Geographic Information Systems in Geological Faults Detection in Crete Island, Greece.

Mohamed Elhag[1*], Dalal Alshamsi[2]

[1] Department of Hydrology and Water Resources Management, Faculty of Meteorology, Environment & Arid Land Agriculture, King Abdulaziz University Jeddah, 21589. Saudi Arabia.

[2] Department of Geology, College of Science, United Arab Emirates University.

**Correspondence to:* melhag@kau.edu.sa

Abstract

Fracture systems are of great importance in the field of structural geology. Faults commonly afford easy passage to groundwater and fluids such as hydrothermal fluids and magmas (mineral entrapment over the years) or even contribute in earthquake hazard monitoring. For a geologist it is not always easy to discern such morphotectonic structures at close range (i.e. heavy overgrowth of vegetation). Both remote sensing techniques and spatial modeling (GIS) permit the recognition and better understanding of the brittle tectonics in an area. This study was an effort to delineate the tectonic structures (i.e. fault system) on the Crete Islands by combining Sentienl-2 satellite data and spatial data. For the enhancement and better discrimination of photolineaments primarily recognized on satellite imagery, a variety of enhancement techniques have been applied. The evaluation of a photolineament as a potential fracture zone was based on several factors; the DEM of the study area, the shaded relief, the slopes and corresponding aspects, the drainage network, the geology and general observations on vegetative coverage appearance. The application of these methods revealed several fracture zones, which we recommend being certified by field investigations. Fault-mapping results may be used for a variety of purposes. Indicative places of large concentration of groundwater are of vital importance for subsequent exploitation by areas of need. Furthermore, because the well-known Anatolian fault zone extends over the Northern part of Crete, the present work may provide useful information for further analysis by geophysists and seismologists.

Keywords: DEM. Fracture Detection, Morphometric, Morphotectonic, Remote Sensing, Photolineaments.

1. Introduction

O' Leary et al. (1976) and Colwell, (1983) gave a good-informing definition of the term lineament. It refers to a mappable, single or composite linear feature of a surface, whose parts are aligned in a rectilinear or slightly curvilinear relationship and which differs distinctly from the pattern of adjacent features and presumably reflects a subsurface phenomenon.

An extensive literature review on the consideration of linear features and lineaments is well presented by Siegal and Gillespie (1980). Suffice to say here, that lineaments identified on aerial photographs and satellite images may represent diverse topographic features (drainage lines), vegetation/soil alignments, coastal lines, crests, ridges, stratigraphic contacts, fold axis (foliation) and seismic zones (Lunkka 1994).

The importance of detecting lineaments lies in the fact that they often represent fault systems. Faults indicate failure of the crust along a surface, accompanied by the relative movement of the geological units from both sides of that surface (Caumon et al. 2009). Such a zone of structural weakness is a major component in structural geology and may be related to a series of other phenomena. It is noticeable that, in many cases in the past, such a system has been related to seismic events occurring in an area. Locating and identifying the movement is of dual importance to a geologist as the impacts of seismic hazards may encompass of both lives and economic losses (Colwell 1983).

Furthermore, faults identification is of economic importance too. That is for; they commonly afford easy passage to several fluids like water, hydrothermal fluids and magmas (Oelkers et al. 2009). Groundwater on the one hand, can be easily transferred through such channel ways, sometimes over large distances and finally reaching and supplying areas of need. On the other hand, mineral entrapping at some time in the past may be of advantageous exploration use (Elhag and Bahrawi 2014).

In the case of faults detection, integration of Remote Sensing and Geographic Information Systems is an issue of great interest. That is for, photolineaments on satellite images do not always account for failure of the crust. They may well represent the drainage lines of the area (rivers), geological boundaries of formations or even cultural features such as roads. The criteria for faults investigation are discussed in several aspects (Greenbaum 1992; Schulson 2004).

Vegetation may play a great role in photogeology for it may reveal underlying structural features not easily discerned at close range. As far as fracturing is concerned, attention should be given to preferential growth of vegetation along linear-curvilinear surfaces (Rodomsky 2011). The reason for this, as mentioned earlier on, is that fractures often act as channel for underground water. Water subsequently, increases the moisture content of soil (in relation to surrounding area) and encourages in one sense, a preferential alignment of vegetation along these fracture zones (Singhal and Gupta 2010). Moreover, it is not rare to identify on an image (or photograph) abrupt changes in types of vegetation or even sudden disappearance of a certain plant species. Particularly in the case where vegetation varies over a surface underlain by the same type of bedrock, fracturing is implied (Phillips et al. 2008).

Faults in some cases, may even throw permeable against impermeable rocks. Water again finds ways along the zone of structural weakness and reaches the Earth's surface by numerous springs (along the contact of the two formations). At these points, high moisture conditions are particularly favorable to intense vegetation growth (Singhal and Gupta 2010).

Abrupt changes in slope are commonly associated with brittle tectonics (Agliardi et al. 2001; Agliardi et al. 2009). Attention should be given though to the orientation of slopes with respect to the illumination source. It may have an impact on vegetation and hence confuse the photointerpreter. As Singhal et al. (2010) pointed out, this factor may greatly influence the survival of plants and explained that moisture content along the surface of a given slope varies. That is for; the parts that are not so well exposed to sun lighting retain less moisture than the more illuminated ones and hence a contrast of low-to-high density vegetation growth occurs.

The knowledge of underlying bedrock type is crucial for the processing of a photogeologist's work. Any truncation and displacement of beds may effectively reveal fracturing (Odling et al. 1999). Abrupt changes in geological formations may also indicate fault zones (Stein 1991). A fault may bring in contact rocks of different petrology and general characteristics that show no physical or inherent association between the two formations. In other words, these formations are not expected to be in contact with each other unless fracturing has occurred at some time in the past (Boggs 2009).

Variations in vegetation discussed above, may be also due to petrological differences of underlying rocks, without necessarily the presence of a fault (Rodomsky 2011). One explanation for such variations is that of bedrock influencing soil composition and consequently the plant species that can exist.

This study was an effort to delineate the brittle tectonics of Crete islands in Kolymvari area (Greece) by using spatial models and digital image processing. The satellite image that was initially provided in the laboratory was enhanced by a variety of methods for the better discrimination of photolineaments. Certainly, not all lineaments detected, were expected to represent failure of the crust (faults) and could be easily confused with roads and rivers. They had to be studied with respect to real-life conditions. In particular, information related to geomorphology (elevation, slopes, aspect, and drainage system) and geology of the region (types of rocks, boundaries of geological formations) was integrated with the satellite data and the final evaluation of a certain lineament, as a potential fault was carried out.

2. Materials and Methods

2.1. Study Area

The hydrological basin of the study area is situated in the western part of Crete Island and is referred to Municipality of Kolymvari (Figure 1). The landscape structure is fundamentally mountainous, resulting in plain only near the coast. The area has a sub-humid Mediterranean climate with an annual average temperature of 19.96°C (Elhag and Bahrawi 2016). The watershed of Kolymvari is mainly an agricultural area where the most common cultivations are olive trees, citrus trees, vineyards, and vegetables. The area has also light industrial activities such as olive mills, wineries, and other agricultural factories. In the coastal zone of Keritis watershed, there are many touristic units (Papafilippaki et al. 2007). However, the possible flow paths were all directed to Kolymvari Stream, which is, therefore, the surface water body (Elhag et al. 2017). From geotectonic point of view, it has not been easy to classify. Lack of fossils in many cases and difficulties in comprehending the exact geo-processes involved in the formation of the Aegean Sea during the Pliocene and Pleistocene, have been an issue under investigation from many geologists over the past years.

2.2. Remote Sensing Data

The goal of digital image processing was to improve such spectral responses and generate images more interpretable than the original ones, where photolineaments would be better

Geosci. Instrum. Method. Data Syst. Discuss., https://doi.org/10.5194/gi-2018-47
Manuscript under review for journal Geosci. Instrum. Method. Data Syst.
Discussion started: 2 October 2018

Geoscientific Instrumentation Methods and Data Systems Discussions
Open Access
EGU

discerned. The digital image of Sentienl-2A (Tile Number: T34SGE, with 0% cloud cover) dating 12/03/2018 and covering the pilot area, has been subject to several enhancement techniques. There were two basic types of distortions that had to be reckoned with, prior to any of the enhancement methods; radiometric distortions and geometric distortions.

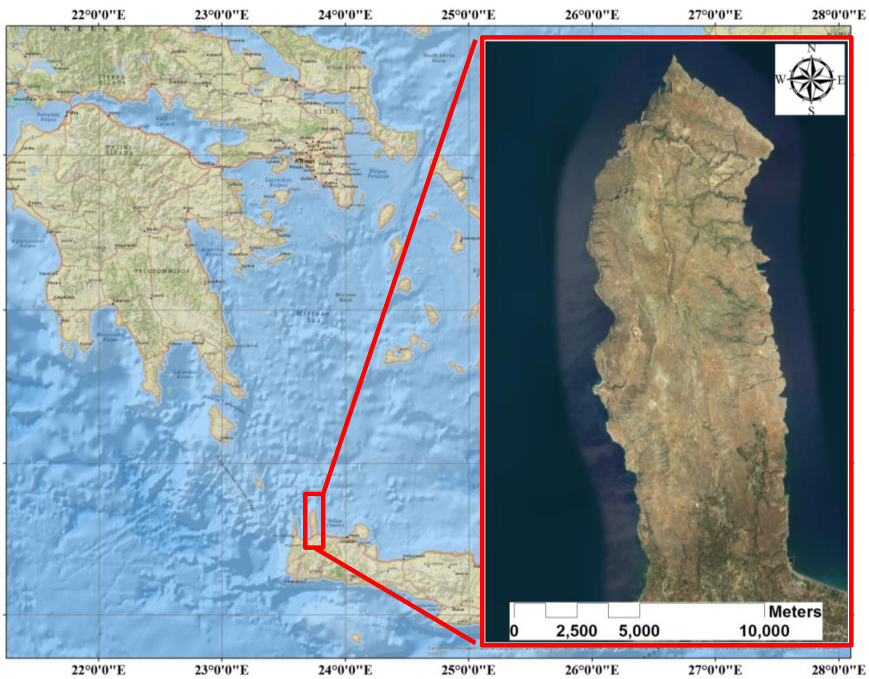

Figure 1. Location of the study area

2.2.1. Lineaments Evaluation by RS means

A variety of enhancement methods have been applied to digital raw data in order to improve the spectral characteristics of objects and emphasize the photolineaments of the area under investigation. The original bands have been contrast-stretched for DNs occupy more gray levels than before, in accordance with their frequency of occurrence (histogram equalize stretching). According to Oskoei and Huosheng (2010), the Isotropic Laplacian, non-directional convolution

Geosci. Instrum. Method. Data Syst. Discuss., https://doi.org/10.5194/gi-2018-47
Manuscript under review for journal Geosci. Instrum. Method. Data Syst.
Discussion started: 2 October 2018

filtering as well as edge-enhancement technique, have been applied to Sentienl-2 (for vegetation and geological features are particularly responsive in these two wavelength bands). Principal Component Analysis aimed to compress information in fewer bands than the original ones, uncorrelated to each other. Images generated by rationing, accounted for the real spectral characteristics and physical properties of objects (topography and illumination effects on the brightness values of pixels, have been eliminated). Schematic flow chart of the implemented procedure in digital image analysis is illustrated in Figure 2.

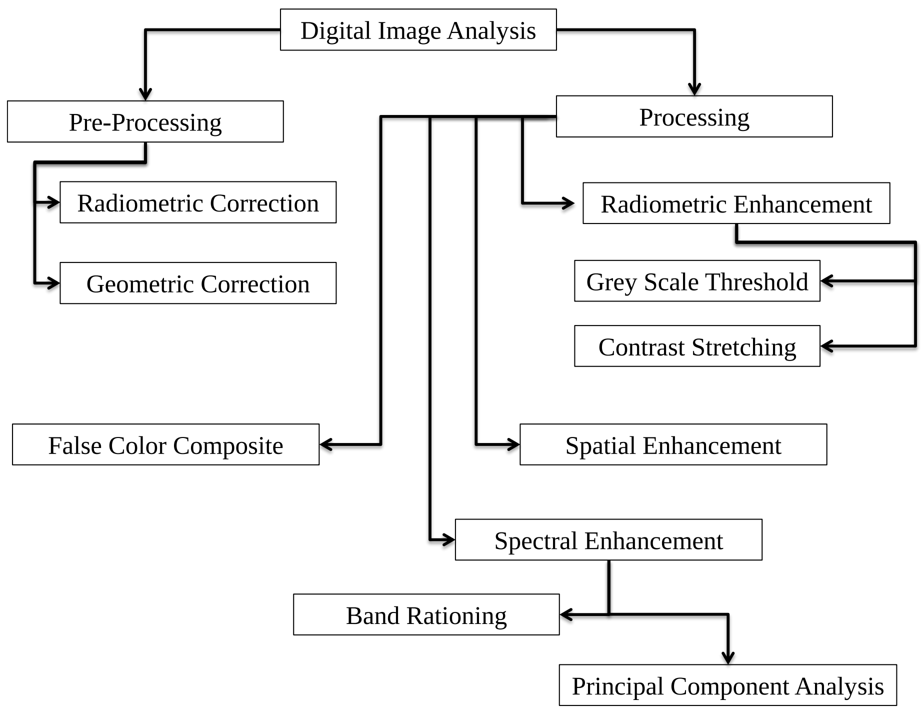

Figure 2. Workflow of Digital Image Analysis

Grey level threshold and Contrast stretching, Sentienl-2, B5 has turned out to be the most appropriate one, for in this near infrared channel, land areas are highly reflected whereas water areas are highly absorbed (Elhag 2017). In 16-bit computer encoding, a digital image can be displayed over a dynamic range of 65536 gray levels (Lillesand et al. 2014). In many cases however, only a small portion of these 65536 levels that are available by devices is utilized. The radiometric ranges (minimum and maximum values of DN values) in each of the six (6) utilized bands (Sentienl-2 B2-B7) of the original dataset are corrected.

Spatial Enhancement, the concept is based on a moving window (the so-called Kernel window) that in short, contains an array of weighting factors, moves successively over all the pixels of a single black and white image (individual band) and ascribes new weighted DN-values as a result of the weighted original ones (Gupta 2017). A high pass filter, in order to emphasize high frequency features or else local spatial detail (Aiazzi et al. 2002). The filter size was 5*5 and was added back to the fourth band of the original band so that low frequency brightness information was not totally lost.

Principal Component Analysis (PCA) is a unique mathematical transformation, designated to reduce such redundancy in multispectral data (Kaarna et al. 2000). The idea is to compress all the information contained in the n-original bands, into fewer than N-new channels/components (Lillesand et al. 2014).

The high interband correlations (very close to 1) suggested that the best way to proceed with this work was by applying a Principal Component Analysis (Table 1). No pair of bands presented covariance =0 i.e. no pair of bands were completely independent to each other. Moreover, as covariance > 0, data appeared to be positively correlated (Elhag 2016).

Rationing, it involves the division as well as more complex functions (additions, subtractions, multiplications) between the DNs of two single bands (Wu et al. 2008). The technique is indicative for both preserving the spectral reflectance characteristics of surficial matter and masking brightness variations derived from illumination conditions and topographic effects (Soulakellis et al. 2006).

Table 1. Interband correlations.

	Band 2	Band 3	Band 4	Band 5	Band 6	Band 7
Band 2	1	0,950535	0,927525	0,244727	0,6878	0,767209418
Band 3	0,950535	1	0,974041	0,406527	0,7474	0,815756429
Band 4	0,927525	0,974041	1	0,418655	0,8131	0,879577936
Band 5	0,244727	0,406527	0,418655	1	0,607	0,468485418
Band 6	0,687812	0,7474	0,813061	0,607007	1	0,956571297
Band 7	0,767209	0,815756	0,879578	0,468485	0,9566	1

False Color Composite (FCC), one band at a time can be displayed in each of the three color-guns; generating false - color composite images (objects do not appear in their natural colors) that are undoubtedly more interpretable to human's eye than black and white images. For the present work several combinations have been tried between original bands, stretched ones, the principal component products as well as the ratio images (Pohl and Van Genderen 1998). The scope was to produce a FCC image where Photolineaments would be discriminated to a satisfactory degree for their further digitizing on screen. Table 2 summaries the used band combinations and its uses.

2.2.2. Lineaments Evaluation by GIS means

Basically, not all photolineaments detected using Remote Sensing techniques are represented as fracturing (Karnieli et al. 1996). Cultural features such as roads had to be readily recognizable on satellite data to avoid their confusion with faults and lead to false photointerpretation results. Schematic flow chart of the implemented procedure in spatial image analysis is illustrated in Figure 3.

Geosci. Instrum. Method. Data Syst. Discuss., https://doi.org/10.5194/gi-2018-47
Manuscript under review for journal Geosci. Instrum. Method. Data Syst.
Discussion started: 2 October 2018

Table 2. False Color Combinations

	Band Combination	Uses
FCC1	B4, B3, B2	Vegetation outcrop in false color composite image appeared red. In cases of preferential vegetation appearance along linear/ curve linear features, potential underlying fracturing.
FCC2	PC1, B4, B2	Geology was not easily discriminated whereas drainage network appeared partially enhanced (bluish tones).
FCC3	PC1, B6, B5	NDVI's contribution in the green color-gun was reflected by the very bright green pixels. No other noteworthy remark could be made. Topography was totally lost.
FCC4	PC1, B4, PC2	Vegetation appeared in bluish tones. The drainage lines in the northern part of the study area were well detected.
FCC5	PC1, B5convolved, B3	No clear discrimination of the geology of the area was achieved.
FCC6	PC1, B5convolved, B7stretched	Less certain discrimination of the geological boundaries/geology of the area. No actual discrimination was made.
FCC7	PC1, PC2, PC3	no prediction of the color characterizing each feature was easily made. The overthrust in the northern part was readily differentiated from the rest of the study area.
FCC8	PC1, PC2, B3	The use of two PCs did not give noteworthy results. Bright green pixels represented vegetative coverage, whereas dark tones of green delineated to a limited extend the drainage network. The elongated feature was not enhanced in this product.
FCC9	PC1, B5convolved, PC3	Topography was better expressed than in the previous case (PC1 in combination with PC2). Several lineaments were readily seen (for non-directional filtering of B5 component).
FCC10	B7enhanced, B5convolved, B3	No particular enhancement was observed compared to the previous products.
FCC11	PC1, B5convolved, B5	Several photolineaments were enhanced, topography was well expressed while stratigraphic contacts were not well delineated.
FCC12	PC1, B5convolved, B3	Partial enhancement of drainage network and preferential alignments of vegetation (greenish tones).
FCC13	PC1, B6, B3	Topographic sense was lost. Some vegetation alignments and abrupt changes in green tonal variations.
FCC14	PC1, B5, B3	topography was very well expressed whereas objects appeared in very natural colors and tones. The drainage network was well delineated, and several lineaments were detected. The same difficulty met in previous combinations in discriminating between the diverse geological formations.

Geosci. Instrum. Method. Data Syst. Discuss., https://doi.org/10.5194/gi-2018-47
Manuscript under review for journal Geosci. Instrum. Method. Data Syst.
Discussion started: 2 October 2018

Geoscientific Instrumentation Methods and Data Systems Discussions
Open Access

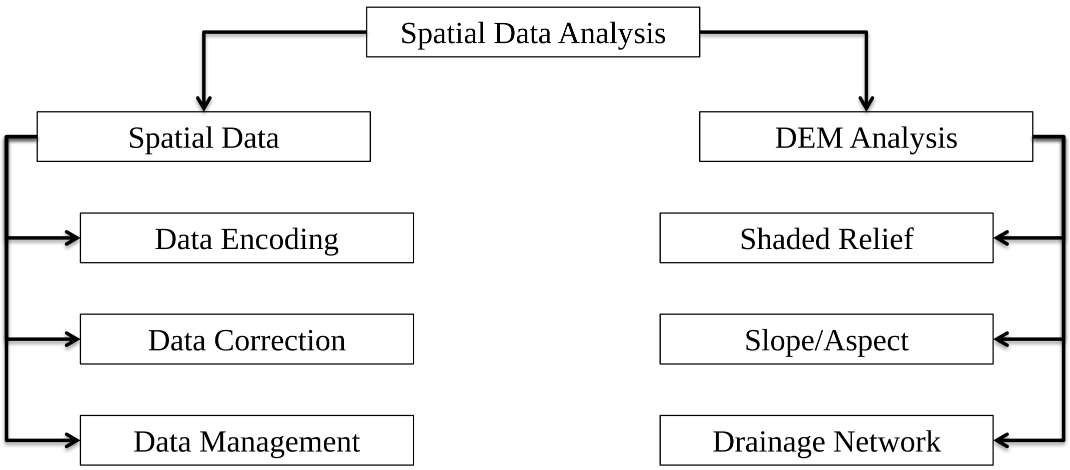

Figure 3. Workflow of Spatial Image Analysis

3. Results and Discussion

3.1. RS Lineaments Evaluation

To transform the original data onto the new PC axes, transformation coefficients (eigenvalues, eigenvectors) should be obtained (Johnson and Wichern 2002). Eigenvalues are presented in Table 3 and describe the variation within the dataset. The % of total scene variance explained by each PC is given by:

(eigenvalue for PCx * 100) / (sum of all eigenvalues)

Table 3. Eigenvalues - % of total variance

PC	Eigenvalue	% of Variance	Cumulative% of Variance
PC1	900.7121015	82.27270992	82.27270992
PC2	124.3086818	11.354585	93.62729492
PC3	58.20089834	5.316177743	98.94347266
PC4	7.348228513	0.671200789	99.61467345
PC5	3.339351294	0.305022526	99.91969598
PC6	0.879159159	0.080304024	100
SUM	1094.788421		

Where x :1,2,3 ... 6

PC1 contains the largest amount of total scene-variance (82, 27%) and hence, is the most correlated component with the original bands. PC2 on the other hand, accounts for a smaller amount of the remaining information (11,35%), PC3 for 5,3% and so on. The three first PCs account for 98, 94% of total scene-variance. As Nikolakopoulos et al. (2008), pointed out, noise is suppressed to the less correlated extracted PCs (Lukáš et al. 2006). Hence, the rest of the principal components (PC4, PC5, PC6) have been ignored.

Eigenvector matrix (Table 4) provides 'us with the loadings or else relative contributions, of each of the bands to each of the PCs.

Table 4. Relative contribution of each band to each extracted PC.

	PC1	PC2	PC3	PC4	PC5	PC6
Band-2	0.256745	-0.43474	-0.45772	0.548567	-0.439	-0.205610634
Band-3	0. 179081	-0.19287	-0.33306	-0.06943	0.1385	0.892072198
Band-4	0.314162	-0.29929	-0.39863	-0.407	0.5738	-0.397391284
Band-5	0.259551	0.80314	-0.51111	-0.0477	-0.147	-0.050194624
Band-6	0.761122	0.122543	0.471784	0.346882	0.2476	0.038391621
Band-7	0.395779	-0.1555	0.19195	-0.63718	-0.613	0.004267441

PC1 has only positive loadings. That means that in the output image no particular feature or structures are expected to be enhanced. It seems that it is a little bit more correlated to Sentinel-2, B7 in comparison with the rest of the bands. PC1 however, bears many similarities to all six bands and can be used as an image of high quality on its own. It is a weighted product of more or less all input images and reflects in a very good way the albedo and topography of the area.

PC2 is a contrast between the high positive loading of Sentinel-2, B5 and the negative loading of Sentinel-2, B2. Hence, PC2 as a single black and white image emphasizes the different sets of features that are sensitive to these bands. More particularly, the spectral responses of the vegetation biomass that is present in the scene (Sentinel-2, B5) contrasted to the soil-vegetation differentiations (Sentinel-2, B2).

As far as PC3 is concerned, the output image is of less significance, as no clear discrimination is available. Information related to the correlation between the bands and the extracted PC's are also given in Table 5. Factor loadings R, were computed in Excel by using the following formula:

R (xp) = eigenvector (xp) * eigenvalue (p) % / variance (x) 1/2

where x refers to the xth channel and p to the pth component (Johnson and Wichern 2002).

Table 5. Factor loadings

	PC1	**PC2**	**PC3**
Band-2	0.778556	-0.48975	-0.35283
Band-3	0.841781	-0.33679	-0.39796
Band-4	0.891965	-0.31568	-0.2877
Band-5	0.623355	0.716576	-0.31203
Band-6	0.985093	0.058921	0. 155217
Band-7	0.968296	-0.14133	0. 119375

The correlation coefficient R extends in a range of -1 to 1. This is nothing more than unit-normalization so that loadings are between -1 and 1 (Johnson and Wichern 2002). The closer the coefficient is to -1 or 1, the more significant is the contribution of a channel to the corresponding PC. Similarly, a loading close to zero is an indication of practically no contribution of a band to the corresponding PC. Thus, PC1 is highly correlated to all bands but mostly to Sentinel-2, B6 and Sentinel-2, B7. PC2 on the other hand, is highly correlated to Sentinel-2, B5 and may be used instead of the latter for a color-composite image.

For vegetation is highly reflected in near infrared and low reflected in visible red, (Sentinel-2, B4)/ (Sentinel-2, B5) ratio generated an image where vegetation appeared in dark tones. In an analogous way, due to the comparatively high reflectance of vegetation in visible green to the lower reflectance in mid infrared, vegetation in (Sentinel-2, B3)/ (Sentinel-2, B6) image appeared in light tones. In both ratios, topography has been eliminated and the area gave the impression of being flat. The two images however, as well as the NDVI product can be safely viewed together for the detection of vegetation biomass. Positive NDVI values, correlate with vegetation while null values correspond to rocks and soil (Johnson and Wichern 2002).

(Sentinel-2, B7) + (Sentinel-2, B4) ratio, was based on an idea to enhance stratigraphic contacts. That is for Sentinel-2, B7 is important in geology for the discrimination of geologic rock type whilst one of Sentinel-2, B4's purposes is the detection of geological boundaries where no particular enhancement was noticeable though.

Efforts to use others than Sentinel-2, B2 band in the ratio applied resulted in negative pixel values (black pixels within the study area) and hence, could not be used for further analysis. In comparison with the rest of the ratios, $((\text{Sentinel-2, B2})^2 + (\text{Sentinel-2, B5})^2)^{1/2}$ product delineated in a better way vegetation amount while several lineaments were emphasized.

Edge enhancement methods resulted in the enhancement of individual bands (black and white images) to a satisfactory degree. However, due to the low capability of human's eye to discern the slight spectral responses of objects in gray scaling, the need for multispectral imagery (display of more than one bands at a time) resulted in the creation of False Color Composite products (FCC).

A variety of RGB combinations have been tested. FCC14 however, appeared to be the most appropriate one for photolineaments discrimination. PC1 accounted for topography (essential element in photointerpretation) whereas R5 reflected the spectral characteristics of vegetation amount (for Sentinel-2, B5 component of ratio R5). Unfortunately, despite the contribution of Sentinel-2, B7 in the same ratio, stratigraphic contacts were not easily detected except for FCC14 for the area under investigation.

3.2. GIS Lineaments Evaluation

The height values were divided in 15 classes and then coded in colors in order to better highlight the relief. The artificial illumination of DEM was from a Northwest direction (315°) and from 45° altitude. From statistical point of view, almost one third (1/3) of the area is characterized by slopes less than 8.7° whilst only 4,8% accounts for slopes >43°. As far as the orientation of slopes is concerned, very few surfaces have a northern-northeastern tendency. The scenery denotes all kinds of aspect of slopes.

The geology of the area under investigation with the potential tectonics as resulted from the integration of the enhanced satellite data and the spatial information. The corresponding area show that most of the faults detected on FCC 14 (Figure 4) have been already mapped whereas several more apply for field cross-checking. The integration of Remote Sensing and Geographic Information Systems has proven to be a reliable. method of fault mapping to a satisfactory degree. Only at one side of the mainstream, smaller tributaries develop, which is a very good example of such a valley is presented while the relative displacement of beds at the sides of the streamline, safely enhances the suspicion of underlying fracturing.

Geosci. Instrum. Method. Data Syst. Discuss., https://doi.org/10.5194/gi-2018-47
Manuscript under review for journal Geosci. Instrum. Method. Data Syst.
Discussion started: 2 October 2018

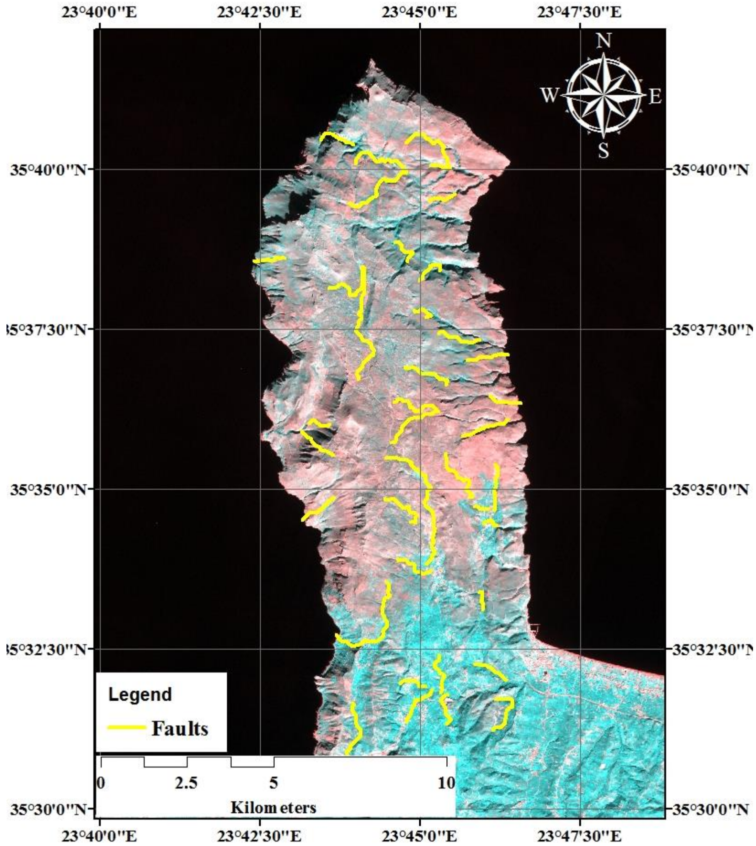

Figure 4. Fault detection using False Color Composition FCC14

Further extended fault zone recognized in the study area. It is the same feature observed in all cases of digital image enhancement. The streamline following it, implies underlying fracturing. A part of this zone has been already mapped. It is clear though, that the zone extends over a larger area than the one found and mapped during field investigations.

Several more examples that enforced the belief of underlying failure as was initially suspected during photointerpretation, and undoubtedly the drainage network has proven to be an indispensable tool in the evaluation of photolineaments.

The final FCC14 that was used for photolineaments detection was composed of PC1, R5 and Sentinel-2, B3 in Red, Green and Blue respectively. R5 on the other hand was a complex function between Sentinel-2, B5 and Sentinel-2, B7. Sentinel-2, B5 is widely used for vegetation amount investigations whilst Sentinel-2, B7 is very common in the field of Geology. Hence, the variant tones of green in FCC14 would normally account for vegetation and/or geology. Since the map of geology of the area was already in hand, in digital form no confusion was made. In some cases, vegetation alignment could safely reveal underlying structural weakness whereas in other cases, truncation and displacement of beds were sufficient for the evaluation of the lineament concerned. Particular attention was paid when a particular lineament connected to a geological boundary.

In order to evaluate the photolineaments detected on FCC14 as indicators of underlying structural weakness, certain phenomena accompanying fracture zones had to be reckoned with. Spatial models (GIS) enabled such estimations. Abrupt changes of slope and aspect, streamline sudden bends and straight segments of streams were the criteria used in general terms. Vegetation alignments and drag effects as were identified during photointerpretation, also applied for a few more lineaments to be recognized. The results of faults detection on FCC14 by Remote Sensing and GIS means whereas the differences between the results derived during this work and conventional fault-mapping (during fieldwork) can be noticed.

4. Conclusions

Beyond a reasonable doubt, the integration of Remote Sensing and Geographic Information Systems (GIS) in the · case of fault detection in designated study area gave satisfactory results. A variety of enhancement techniques resulted in the discrimination of several photolineaments. Not all of them related to fracturing. Cultural features such as roads were immediately extracted so that no confusion would be made with faults. The same was true for drainage lines and geological boundaries, which in many cases were strongly emphasized and could easily result in false identification.

The best combination has proven to be for the first Principal Component (PC1 in red color-gun, accounting for 82.27% of total scene variance), ratio product R5 = $((\text{Sentinel-2, B5})^2 + (\text{Sentinel-2, B7})^2)^{1/2}$, and one of the original bands (Sentinel-2, B3). For Sentinel-2, B5's contribution in R5, the spectral characteristics of vegetation amount were emphasized (vegetation is particularly responsive in Sentinel-2, B5). Hence, the preferential growth of vegetation along linear features, suggested in many cases underlying fracturing. Despite Sentinel-2, B7's contribution in the same ratio, the spectral responses of geological formations were not highlighted except for very few cases of apparent displacement of beds. PC1 on the other hand accounted for the topographic information that was lost due to ratio's contribution.

Spatial modeling (DEM and products) was crucial for the evaluation of photolineaments detected on FCC14 (PC1, R5, in Sentinel-2, B3). The Digital Elevation Model of the area under investigation and the derived maps of slope and aspect enabled several times to imply for fracturing (wherever abrupt changes of slope and aspect were observed at the sides of a particular photolineament).

The drainage network has proven to be particularly helpful and informative on the underlying structures. Rift valleys and displacement of rivers' routes were common phenomena within the scene of observation. In many cases parallel vegetation alignments differing from the vegetation outcrop of the surrounding area (abrupt tonal differences) further assured us about possible failure of the crust. Of course, the analysis was not based on the number of criteria satisfied each time. A fault associated with more criteria than another does not necessarily make it a fracture zone of more significance.

In comparison with the conventional methods of mapping (field investigations) most of the faults recognized by automated watershed delineation, have already been mapped during field investigations. Several of the zones found, were not discerned on the FCC14. That was due to the following parameters that someone needs to bear always in mind before proceeding with analogous to the present researches.

Faults mapping by using satellite data integrated with spatial information (GIS), may lead to quite noteworthy results. Experience is crucial for an accurate photointerpretation. In this case study, most of the faults that have been mapped in the past during fieldwork investigations were also identified on the satellite image. Some of the photolineaments discerned but were not readily seen on FCC14. That should be for all factors explained earlier on. Lastly, for all photolineaments that were identified on the satellite image and raised suspicion of failure of the crust, in- situ data collection for verification of the results is strongly recommended, in order to be total aware of the tectonics of the area.

References

Agliardi, F, G Crosta, and A Zanchi. 2001. 'Structural constraints on deep-seated slope deformation kinematics', *Engineering Geology*, 59: 83-102.

Agliardi, Federico, Andrea Zanchi, and Giovanni B Crosta. 2009. 'Tectonic vs. gravitational morphostructures in the central Eastern Alps (Italy): constraints on the recent evolution of the mountain range', *Tectonophysics*, 474: 250-70.

Aiazzi, Bruno, Luciano Alparone, Stefano Baronti, and Andrea Garzelli. 2002. 'Context-driven fusion of high spatial and spectral resolution images based on oversampled multiresolution analysis', *IEEE transactions on Geoscience and Remote Sensing*, 40: 2300-12.

Boggs, Sam. 2009. *Petrology of sedimentary rocks* (Cambridge University Press).

Caumon, G, P Collon-Drouaillet, C Le Carlier De Veslud, S Viseur, and J Sausse. 2009. 'Surface-based 3D modeling of geological structures', *Mathematical Geosciences*, 41: 927-45.

Colwell, Robert N. 1983. *Manual of remote sensing* (American Society of Photogrammetry).

Elhag, M., and J. A. Bahrawi. 2014. 'Conservational use of remote sensing techniques for a novel rainwater harvesting in arid environment', *Environmental Earth Sciences*, 72: 4995-5005.

———. 2016. 'Deliberation of Hilly Areas for Water Harvesting Application in Western Crete, Greece', *GLOBAL NEST JOURNAL*, 18: 621-29.

Elhag, Mohamed. 2016. 'Evaluation of different soil salinity mapping using remote sensing techniques in arid ecosystems, Saudi Arabia', *Journal of Sensors*, 2016.

———. 2017. 'Consideration of Landsat-8 Spectral Band Combination in Typical Mediterranean Forest Classification in Halkidiki, Greece', *Open Geosciences*, 9: 468-79.

Elhag, Mohamed, Jarbou A Bahrawi, Hanaa K Galal, Amal Aldhebiani, and Amal AM Al-Ghamdi. 2017. 'Stream network pollution by olive oil wastewater risk assessment in Crete, Greece', *Environmental Earth Sciences*, 76: 278.

Greenbaum, D. 1992. 'Structural influences on the occurrence of groundwater in SE Zimbabwe', *Geological Society, London, Special Publications*, 66: 77-85.

Gupta, Ravi P. 2017. *Remote sensing geology* (Springer).

Johnson, Richard A, and Dean Wichern. 2002. *Multivariate analysis* (Wiley Online Library).

Kaarna, Arto, Pavel Zemcik, Heikki Kalviainen, and Jussi Parkkinen. 2000. 'Compression of multispectral remote sensing images using clustering and spectral reduction', *IEEE transactions on Geoscience and Remote Sensing*, 38: 1073-82.

Karnieli, Arnon, Amnon Meisels, Leonid Fisher, and Yaacov Arkin. 1996. 'Automatic extraction and evaluation of geological linear features from digital remote sensing data using a Hough transform', *Photogrammetric engineering and remote sensing*, 62: 525-31.

Lillesand, Thomas, Ralph W Kiefer, and Jonathan Chipman. 2014. *Remote sensing and image interpretation* (John Wiley & Sons).

Lukáš, Jan, Jessica Fridrich, and Miroslav Goljan. 2006. "Detecting digital image forgeries using sensor pattern noise." In *Security, Steganography, and Watermarking of Multimedia Contents VIII*, 60720Y. International Society for Optics and Photonics.

Lunkka, Juha Pekka. 1994. 'Sedimentation and Iithostratigraphy of the North Sea Drift and Lowestoft Till Formations in the Coastal cliffs of northeast Norfolk, England', *Journal of Quaternary Science*, 9: 209-33.

Nikolakopoulos, Konstantinos G, Panagiotis I Tsombos, George Aim Skianis, and Dimitrios A Vaiopoulos. 2008. "EO-1 Hyperion and ALI bands simulation to Landat 7 ETM+ bands for mineral mapping in Milos Island." In *Remote Sensing for Environmental Monitoring, GIS Applications, and Geology VIII*, 711010. International Society for Optics and Photonics.

O'leary, DW, JD Friedman, and HA Pohn. 1976. 'Lineament, linear, lineation: some proposed new standards for old terms', *Geological Society of America Bulletin*, 87: 1463-69.

Odling, NE, P Gillespie, B Bourgine, C Castaing, JP Chiles, NP Christensen, E Fillion, A Genter, C Olsen, and L Thrane. 1999. 'Variations in fracture system geometry and their implications for fluid flow in fractures hydrocarbon reservoirs', *Petroleum Geoscience*, 5: 373-84.

Oelkers, Eric H, Pascale Bénézeth, and Gleb S Pokrovski. 2009. 'Thermodynamic databases for water-rock interaction', *Reviews in Mineralogy and Geochemistry*, 70: 1-46.

Oskoei, Mohammadreza Asghari, and Huosheng Hu. 2010. 'A survey on edge detection methods', *University of Essex: Essex, UK*.

Papafilippaki, A, D Gasparatos, C Haidouti, and G Stavroulakis. 2007. 'Total and bioavailable forms of Cu, Zn, Pb and Cr in agricultural soils: A study from the hydrological basin of Keritis, Chania, Greece', *Global Nest J*, 9: 201.

Phillips, Jonathan D, Daniel A Marion, and Alice V Turkington. 2008. 'Pedologic and geomorphic impacts of a tornado blowdown event in a mixed pine-hardwood forest', *Catena*, 75: 278-87.

Pohl, Cle, and John L Van Genderen. 1998. 'Review article multisensor image fusion in remote sensing: concepts, methods and applications', *International Journal of Remote Sensing*, 19: 823-54.

Rodomsky, Brett Thomas. 2011. *Lava roughness, aridity, and early ecosystem development across a topo-climatic gradient: The 1855–56 Mauna Loa lava flow, Hawaii* (University of Hawai'i at Hilo).

Schulson, Erland M. 2004. 'Compressive shear faults within arctic sea ice: Fracture on scales large and small', *Journal of Geophysical Research: Oceans*, 109.

Siegal, Barry S, and Alan R Gillespie. 1980. *Remote sensing in geology* (Wiley New York).

Singhal, Brij Bhusan Saran, and Ravi P Gupta. 2010. *Applied hydrogeology of fractured rocks* (Springer Science & Business Media).

Soulakellis, Nikolaos A, Irwin D Novak, Nikolaos Zouros, Paul Lowman, and Jacob Yates. 2006. 'Fusing Landsat-5/TM Imagery and Shaded Relief Maps in Tectonic and Geomorphic Mapping', *Photogrammetric Engineering & Remote Sensing*, 72: 693-700.

Stein, Carol A. 1991. 'The solid earth: an introduction to global geophysics', *Eos, Transactions American Geophysical Union*, 72: 427-28.

Wu, Jindong, Marvin E Bauer, Dong Wang, and Steven M Manson. 2008. 'A comparison of illumination geometry-based methods for topographic correction of QuickBird images of an undulant area', *ISPRS Journal of Photogrammetry and Remote Sensing*, 63: 223-36.